Turbulent Fluctuations in TFTR Configurations with Reversed Magnetic Shear

E. Mazzucato,[1] S. H. Batha,[2] M. Beer,[1] M. Bell,[1] R. E. Bell,[1] R. V. Budny,[1] C. Bush,[3] T. S. Hahm,[1] G. W. Hammett,[1] F. M. Levinton,[2] R. Nazikian,[1] H. Park,[1] G. Rewoldt,[1] G. L. Schmidt,[1] E. J. Synakowski,[1] W. M. Tang,[1] G. Taylor,[1] and M. C. Zarnstorff[1]

[1]*Princeton Plasma Physics Laboratory, Princeton, New Jersey 08543*
[2]*Fusion Physics and Technology, Torrance, California 90503*
[3]*Oak Ridge National Laboratory, Oak Ridge, Tennessee 37831*

(Received 26 April 1996)

Turbulent fluctuations in plasmas with reversed magnetic shear have been investigated on the Tokamak Fusion Test Reactor. Under intense auxiliary heating, these plasmas are observed to bifurcate into two states with different transport properties. In the state with better confinement, it has been found that the level of fluctuations is very small throughout most of the region with negative shear. By contrast, the state with lower confinement is characterized by large bursts of fluctuations which suggest a competition between the driving and the suppression of turbulence. These results are consistent with the suppression of turbulence by the $\mathbf{E} \times \mathbf{B}$ velocity shear. [S0031-9007(96)01312-9]

PACS numbers: 52.55.Fa, 52.30.Bt, 52.35.Ra

Recent results [1–4] point to the beneficial effects of negative magnetic shear on plasma performance in tokamaks. In these experiments, magnetic configurations with a nonmonotonic safety factor q have been obtained using a variety of techniques. The common result is a strong peaking of the pressure profile which indicates a reduction of plasma transport in the central region with negative shear. Since short scale turbulence is frequently considered to be the source of anomalous losses in tokamaks, these results appear to be consistent with theoretical predictions that negative shear can suppress geodesic curvature driven microinstabilities, such as trapped particle modes [5], the toroidal ion temperature gradient mode [6], and high-n ballooning modes [7].

To study the effects of negative magnetic shear on plasma turbulence in tokamaks, we have conducted an experimental study of turbulent fluctuations in plasmas with reversed magnetic shear on the Tokamak Fusion Test Reactor (TFTR). These are deuterium plasmas with a major radius $R = 2.6$ m, a minor radius $a = 0.94$ m, a toroidal magnetic field $B = 4.6$ T, and a plasma current $I_p = 1.6$ MA. The central plasma region with negative shear is created early in the discharge by a combination of heating and current drive. Under intense auxiliary heating with neutral beam injection (NBI), these plasmas are observed to bifurcate into two different states, the reversed shear (RS) and the enhanced reversed shear (ERS) mode [3]. The RS mode is similar to the *supershot regime* which is normally observed in TFTR with monotonic q profiles. The ERS mode is characterized by highly peaked density and plasma pressure profiles which indicate the formation of a transport barrier (Fig. 1). Since at the time of bifurcation ($t \approx 2.65$ s) the q profiles are very similar in the two plasma modes (Fig. 1), the observed phenomenon cannot be ascribed solely to the negative magnetic shear.

A transport analysis, ignoring particle pinches, gives the electron particle diffusivity (D_e) and the ion thermal conductivity (χ_i) of Fig. 2, which shows a greatly reduced plasma transport in the ERS mode. In particular, the precipitous drop of χ_i inside the reversed shear region to values below those of conventional neoclassical theory [3] reveals the formation of a transport barrier. This improvement of the ion thermal transport in the ERS mode derives from the ion temperature which remains larger than in the RS mode (Fig. 1) in spite of a stronger ion-electron coupling.

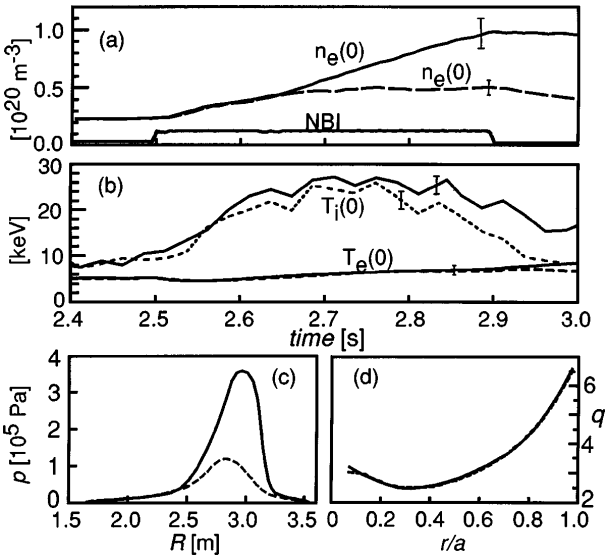

FIG. 1. Time evolution of central electron density (a) and temperatures (b) in ERS (solid line) and RS (dashed line) plasmas with 29 and 27 MW of balanced NBI, respectively. The bottom graphs show the radial profiles of the plasma pressure (c) at $t = 2.9$ s, and the safety factor (d) at the bifurcation time ($t \approx 2.65$ s).

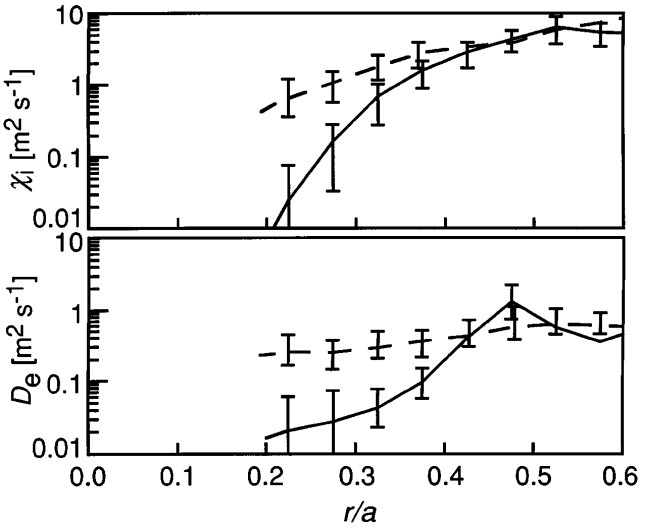

FIG. 2. Electron diffusivity (D_e) and ion thermal conductivity (χ_i) in the ERS (solid line) and RS (dashed line) plasmas of Fig. 1 at $t = 2.75$ s.

The short scale turbulent fluctuations of these plasmas have been investigated with microwave reflectometry. The reflectometer system operated in the X-mode on the frequency range 123–142 GHz. Well collimated beams with a diameter of $\approx$5 cm were launched into the plasma using scalar guides and Gaussian optics.

The interpretation of reflectometry measurements is relatively simple when the amplitude of plasma fluctuations is small and their scale length is larger than the wavelength of the probing wave [8,9]. The latter assumption is satisfied in TFTR where the wave number of previously observed fluctuations is ≈ 1 cm^{-1} [8,10]. This allows the use of the geometrical optics approximation and guarantees that the effects of turbulent fluctuations on the probing wave come predominantly from a narrow region near the cutoff ($\ll$1 cm). At very small levels of fluctuation, the electromagnetic field can be separated into a large coherent reflection and small amplitude scattered waves (Born approximation) [9]. Under these conditions, the level of density fluctuations can be inferred from either the fluctuations in the phase of the received signal or from the ratio between the power of the scattered waves and the power of the coherent reflection. Unfortunately, the first method is of limited use in tokamaks because, as the level of fluctuations increases and the scattered waves rise in amplitude and angular divergence, a complicated interference pattern makes the phase of the received signal completely chaotic and, therefore, useless for fluctuations measurements [11]. The second method has a wider range of applicability [8,11], but it too breaks down when the amplitude of the coherent reflection decreases below detectable levels. This sets the maximum value of measurable density fluctuations, which in the present experiment is in the range $\tilde{n}_e/n_e \approx (0.5\text{–}1.0) \times 10^{-2}$.

Figure 3 shows the time evolution of $\tilde{n}_e/n_e$ at two radial locations inside the negative shear region of the ERS plasma of Fig. 1. From these results, it appears

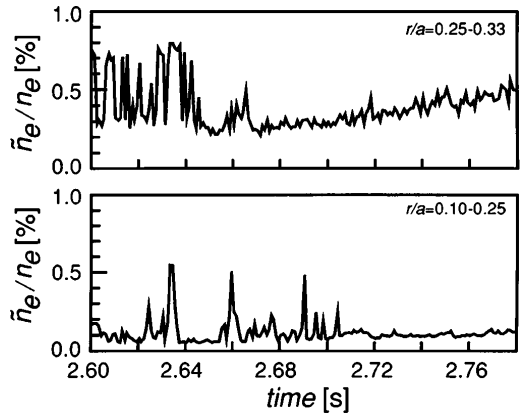

FIG. 3. Time evolution of density fluctuations in the ERS mode.

that large bursts of turbulence which are present before the bifurcation disappear after the transition into the ERS mode. By using the displacement of the probing wave reflecting point which is caused by the plasma density rise, we obtain the amplitude of density fluctuation as a function of the normalized minor radius (r/a) shown in Fig. 4 at $t = 2.72$–2.78 s. Thereafter the profile remains unchanged until the end of the NBI pulse. The abscissa in Fig. 4 are the calculated positions of the reflecting cutoff which include a relativistic correction [12] ranging from 2 to 6 cm. As described elsewhere [8], to obtain the value of $\tilde{n}_e/n_e$ from reflectometry measurements requires a knowledge of the shape of the radial spectrum of fluctuations. Unfortunately, in the rapidly evolving plasmas of the present experiment, this is difficult to measure by performing radial correlation measurements. Nevertheless, all previous theoretical and experimental studies of short scale fluctuations in large tokamaks indicate that the bulk of the turbulent activity occurs at wavelengths larger than the ion Larmor radius (ρ_i), typically in the range of radial wave numbers $0.2 < k_r\rho_i < 1$. Accordingly, the values in Figs. 3–5 have been obtained assuming $k_r = 1$ cm^{-1}, which corresponds to $k_r\rho_i \approx 0.5$, and we have calculated the error bars in Fig. 4 by taking the extreme values of $k_r\rho_i = 0.2$ and 1, respectively. In spite of these uncertainties, from

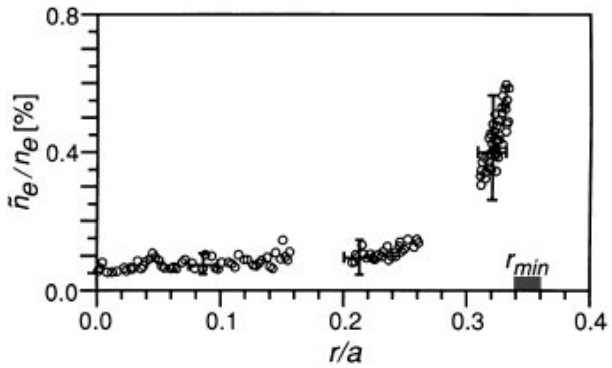

FIG. 4. Amplitude of density fluctuations in the ERS mode at $t = 2.72$–2.78 s; $r_{\min}$ is the radial position with minimum q.

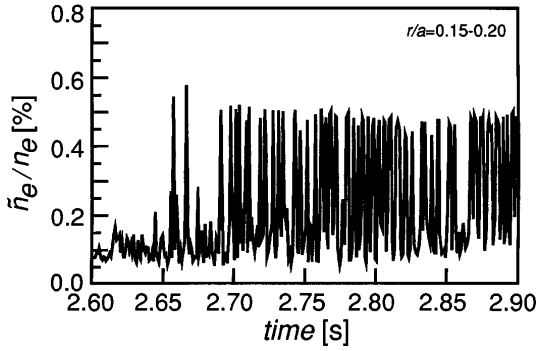

FIG. 5. Time evolution of density fluctuations in the RS mode.

Fig. 4 we can draw the conclusion that the amplitude of fluctuations is very small in the main core of ERS plasmas and that the level of turbulence rises near the point where q reaches its minimum value. Both of these phenomena are reminiscent of the radial dependence of the transport coefficients in the ERS mode (Fig. 2).

Turbulent fluctuations in the RS mode are substantially different from those in the ERS mode, as illustrated in Fig. 5, which shows the time evolution of the fluctuation amplitude in the middle of the negative shear region ($r/a = 0.15$–0.20). From these data, it appears that bursts of turbulence, reaching the maximum detectable level, persist throughout the entire plasma pulse. At larger radii ($r/a > 0.2$), these bursts intensify and become a continuum, while closer to the plasma center ($r/a < 0.1$), the measured level of turbulence is similar to that in the ERS mode. This indicates that a central quiescent region exists in the RS mode as well, but with a much smaller radial extent than in the ERS mode.

To confirm that the observed bursting of turbulence is not an instrumental effect, we have performed a series of tests. As mentioned earlier, large plasma fluctuations have the effect of broadening the spectrum of scattered waves which results in an increase in their angular divergence. When the latter becomes larger than the receiver acceptance angle, a drop in the measured signal power must be observed. This phenomenon is illustrated in Fig. 6, which shows that each burst of turbulence coincides with a drop in the signal power. From the required condition for this

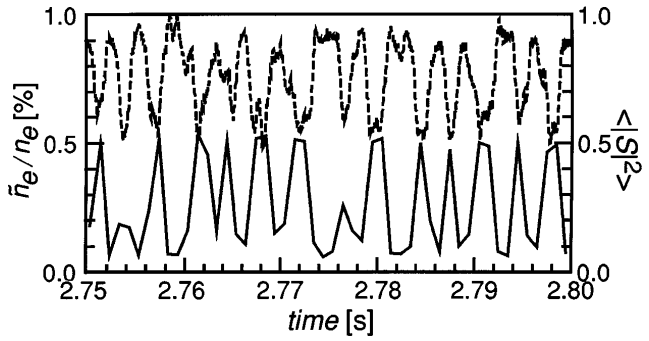

FIG. 6. Time evolution of density fluctuations $\tilde{n}_e/n_e$ (solid line) and total signal power $\langle|S|^2\rangle$ (dashed line) in the RS mode.

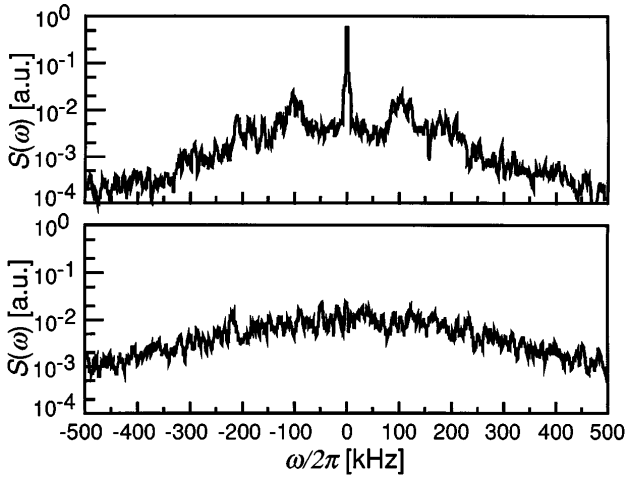

FIG. 7. Power spectrum of measured signals before (top) and during (bottom) a burst of turbulence.

phenomenon to occur, we estimate that the poloidal wave number is in the range $k_\theta = 0.5$–$1.0\ \mathrm{cm}^{-1}$. Another effect of large fluctuations is the disappearance of the coherent reflection. This is illustrated in Fig. 7, which shows the frequency spectrum of scattered waves before and during the burst. The coherent reflection, which in these spectra is represented by the zero frequency component, is clearly absent during the burst. The same phenomenon can be detected on the signal phase, as shown in Fig. 8. Again, while only small fluctuations are visible before and after the burst, the phase becomes completely chaotic during the burst of turbulence, and it displays a large secular drift. The latter is caused by an unbalanced sampling of the wave sidebands which is due to a small misalignment in the reflectometer geometry. In conclusion, all measurements point to a bursting behavior of turbulence which suggests a competition between the driving and the suppression of turbulence [13]. These observations are reminiscent of the bursts of fluctuations which have been detected at the edge of plasmas in the H mode [14,15]. Considering the drastic differences between these plasmas and those of the present experiment with respect to ion temperature (2 vs 25 keV), location (edge vs main core), magnetic shear (positive vs negative), and plasma shape

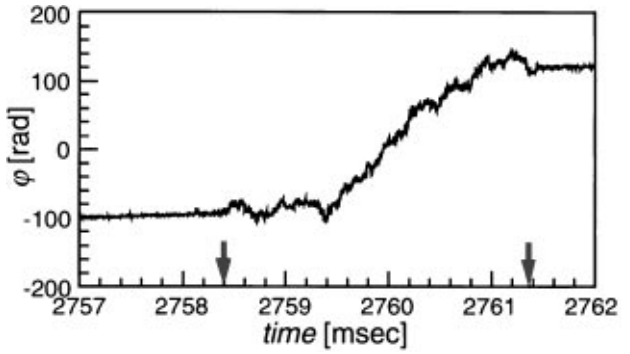

FIG. 8. Phase of measured signal. Arrows mark the beginning and the end of a burst of turbulence.

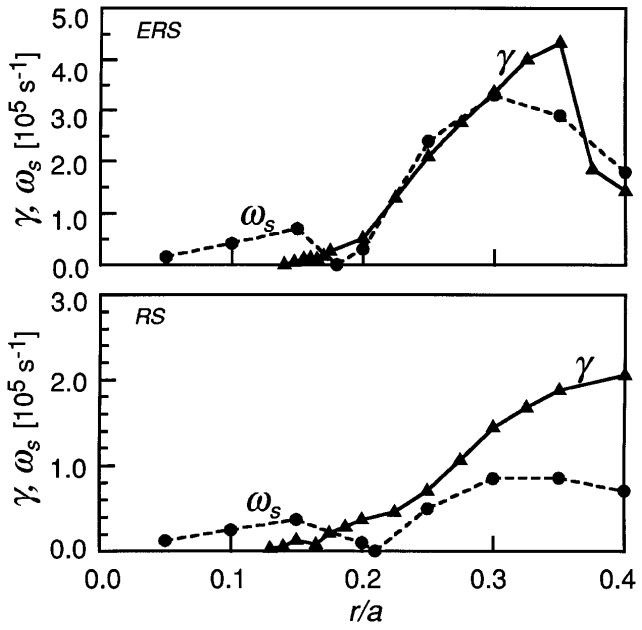

FIG. 9. Calculated values of the maximum linear growth rate γ (triangles, solid line), and the shearing rate ω_s (circles, dashed line) at $t = 2.75$ s. Top is ERS mode, bottom is RS mode.

(D shape vs circular), one might be tempted to speculate that the bursting of turbulence is a characteristic feature of transport barriers in tokamaks.

We have compared our experimental observations with the theoretical predictions for toroidal electrostatic drift-type modes. Figure 9 shows the results for the maximum linear growth rate γ which was obtained with a kinetic toroidal eigenvalue code [16]. Surprisingly, we find the largest values of γ in the ERS mode, which provides further evidence that shear reversal is not the only cause of turbulence suppression in these plasmas. Furthermore, the size of the central stable region is the same in both plasma regimes. These results, which were confirmed by those obtained with a toroidal gyrofluid code [17], demonstrate that other phenomena, besides the reversed shear, play a role in the ERS and RS dynamics.

A possible mechanism for the suppression of turbulence is the decorrelation of turbulent fluctuations by a large $\mathbf{E} \times \mathbf{B}$ velocity shear which may exist in regions of large pressure gradient [18–25]. This mechanism, which in the past has been invoked for explaining the reduction in the level of fluctuations at the edge of the plasmas in the H mode [18,22], might also be at work in the central plasma region with negative magnetic shear [23–25]. The numerical simulations in Ref. [23] indicate that the turbulence is suppressed when the linear growth rate of the most unstable mode (γ) is not larger than a characteristic $\mathbf{E} \times \mathbf{B}$ shearing rate ω_s. For this, we use the expression derived in Ref. [24] which, on the tokamak midplane, gives $\omega_s \approx |(RB_\theta/B)\partial(E_r/RB_\theta)/\partial R|$, where B_θ is the poloidal magnetic field and E_r is the radial electric field which can be obtained by solving the full set of momentum balance equations for multiple species [26]. For the ERS mode, we get $\omega_s \geq \gamma$ over most of the reversed shear region with $\gamma > 0$, while for the RS mode we obtain $\gamma > \omega_s$ over the entire unstable portion of the negative shear region (Fig. 9). From these results, we draw the conclusion that the observed reduction of fluctuations in the ERS mode is consistent with the suppression of turbulence by the $\mathbf{E} \times \mathbf{B}$ velocity shear.

In conclusion, the results presented in this paper provide the first experimental evidence of the correlation between a low level of turbulent fluctuations and the improved confinement in the main core of plasmas with reversed magnetic shear (ERS). We have also detected large bursts of fluctuations in plasmas with a similar reversed magnetic shear but with poorer confinement (RS). These observations, which cannot be explained with numerical results from two linear stability codes, are consistent with the suppression of turbulence by the $\mathbf{E} \times \mathbf{B}$ velocity shear.

The authors are grateful to the TFTR group for the operation of these experiments, and to R. J. Hawryluk for his constant encouragement. This work was supported by U.S. Department of Energy Contract No. DE-AC02-76-CHO3073.

[1] M. Hugon *et al.*, Nucl. Fusion **32**, 33 (1992).
[2] E. A. Lazarus *et al.*, Phys. Fluids B **4**, 3644 (1992).
[3] F. M. Levinton *et al.*, Phys. Rev. Lett. **75**, 4417 (1995).
[4] E. J. Strait *et al.*, Phys. Rev. Lett. **75**, 4421 (1995).
[5] B. B. Kadomtsev and O. P. Pogutse, Sov. Phys. JETP **24**, 1172 (1967).
[6] B. Coppi *et al.*, Phys. Fluids **10**, 582 (1967).
[7] M. S. Chance and J. M. Green, Nucl. Fusion **21**, 453 (1981).
[8] E. Mazzucato and R. Nazikian, Phys. Rev. Lett. **71**, 1840 (1993).
[9] E. Mazzucato and R. Nazikian, Plasma Phys. Controlled Fusion **33**, 261 (1991).
[10] R. Fonck *et al.*, Phys. Rev. Lett. **70**, 3736 (1993).
[11] R. Nazikian and E. Mazzucato, Rev. Sci. Instrum. **66**, 392 (1995).
[12] E. Mazzucato, Phys. Fluids B **4**, 3460 (1992).
[13] B. A. Carreras *et al.*, Phys. Plasmas **2**, 2744 (1995).
[14] C. L. Rettig *et al.*, Plasma Phys. Controlled Fusion **36**, A207 (1994).
[15] T. H. Osborne *et al.*, Nucl. Fusion **35**, 23 (1995).
[16] G. Rewoldt *et al.*, Phys. Fluids **30**, 807 (1987).
[17] M. A. Beer, Ph.D. thesis, Princeton University, 1994.
[18] H. Biglari, P. H. Diamond, and P. W. Terry, Phys. Fluids B **2**, 1 (1990).
[19] K. C. Shaing *et al.*, Phys. Fluids B **2**, 1492 (1990).
[20] B. Basu and B. Coppi, Phys. Fluids B **4**, 2817 (1992).
[21] J. Dong and W. Horton, Phys. Fluids B **5**, 1581 (1992).
[22] F. L. Hinton and G. M. Staebler, Phys. Fluids B **5**, 1281 (1993).
[23] R. E. Waltz *et al.*, Phys. Plasmas **1**, 2229 (1994).
[24] T. S. Hahm and K. H. Burrell, Phys. Plasmas **2**, 1648 (1995).
[25] L. L. Lao *et al.*, Phys. Plasmas **3**, 1951 (1996).
[26] S. P. Hirshman and D. J. Sigmar, Nucl. Fusion **21**, 1079 (1981).